DOI 10.5862/JEST.246.6
УДК 621.313

M.A. Shakirov

2*n*T-SHAPED EQUIVALENT CIRCUIT OF A TRANSFORMER COMPRISING *n* WINDINGS

М.А. Шакиров

2*n*T-ОБРАЗНАЯ СХЕМА ЗАМЕЩЕНИЯ ТРАНСФОРМАТОРА, СОДЕРЖАЩЕГО *n* ОБМОТОК

The new detailed 2*n*T-shaped equivalent circuits of a transformer containing n concentric windings, displaying on schematic all magnetic flux between the windings, in the windings, in the elements of the magnetic circuit and between it and the tank in case of saturation of the magnetic circuit is presented. It is based on the idea of stitching the 4*T*-shaped circuit models for two-winding transformers, considered as a unit cell of a more complex 2*n*T-shaped structure. The accuracy of the occurrence in various parts of the magnetic circuit with short-circuit one or more windings of the magnetic super- and counter-fluxes in comparison with the fluxes of idling is confirmed. It is shown that the observation of such anomalous fluxes in the equivalent circuit is possible due to the presence of negative inductances. It is proved that the multi-winding transformer equivalent circuits without negative elements are characterized by a three-diagonal matrix of inductances.

TRANSFORMER; PRIMARY AND SECONDARY WINDINGS; MAGNETIC FLUX; EQUIVALENT CIRCUIT; TREE-WINDING TRANSFORMER; MULTI-WINDING TRANSFORMER; SHORT CIRCUITED; IDLING; COUPLED INDUCTANCE.

Представлены новые развернутые 2*n*Т-образные схемы замещения трансформатора, содержащего *n* концентрических обмоток, с отображением на схемах всех магнитных потоков между обмотками, в самих обмотках, в элементах магнитопровода, а также между ним и баком в случае насыщения магнитопровода. В основу положена идея сшивания 4*T*-образных схемных моделей двухобмоточных трансформаторов, рассматриваемых в качестве элементарных ячеек более сложной 2*n*T-образной структуры. Подтверждена достоверность возникновения в различных частях магнитопровода при коротких замыканиях одной или нескольких обмоток магнитных сверх- и антипотоков в сравнении с потоками холостого хода. Показано, что наблюдение этих аномальных потоков на схеме замещения возможно благодаря присутствию в ней отрицательных индуктивностей. Доказано, что схемы замещения многообмоточного трансформатора без отрицательных элементов характеризуются трехдиагональной матрицей индуктивностей.

ТРАНСФОРМАТОР; ПЕРВИЧНАЯ И ВТОРИЧНАЯ ОБМОТКИ; МАГНИТНЫЙ ПОТОК; СХЕМА ЗАМЕЩЕНИЯ; ТРЕХОБМОТОЧНЫЙ ТРАНСФОРМАТОР; МНОГООБМОТОЧНЫЙ ТРАНСФОРМАТОР; КОРОТКОЕ ЗАМЫКАНИЕ; ХОЛОСТОЙ ХОД; ВЗАИМНАЯ ИНДУКТИВНОСТЬ.

Introduction

A multi-winding transformer is defined as the one with more than two electrically disconnected windings. Such a transformer can replace two or several double-winding ones, which simplifies the connection between the electric stations and the distribution networks and, in general, results in reducing the maintenance costs and the total costs of electric power systems. However, the correct conclusion

about the benefits of multi-winding transformers (these also include split-winding transformers) can be made only by understanding the complete picture of the physical processes occurring in these transformers, which have not been clarified up to the present time. A discussion unfolded about the main feature of any of their equivalent circuits (polygonal-type [1-5], tree-type [6], chain-type [1,6], etc.), that is, of the negative inductances present in them, which has been cause for alarmist statements such as "there is no reason to look for a physical explanation of this phenomenon..." (see p. 56 in [4]). Ref. [5, p. 124] described the negative inductances as a mathematical curiosity "due to difference between the RMS and the mean values of the function". Ref. [6, p. 89] even went as far as to state that these "inductances have no physical meaning", and the explanation given for their presence is rather nonsensical: "they merely coordinate the equivalent circuit with the existing couplings". The negative inductances are described in this same vein in all textbooks, and their low numerical value in comparison with other inductances is emphasized [7–10]. Despite this, A.Boyjian "physically interpreted them as a result of mutual-inductance coupling" [3]. Following this study, the authors of [11, 12] made a critical review of the papers on the subject and offered to dispose of these 'virtual' values (as described in [3]) by introducing mutual-inductance couplings ($M_{i,j}$) between *all* leakage inductances. Speaking of the three-winding transformer, the authors of [12] write, "we **postulate** that L_{12} and L_{23} must be mutually coupled ", giving a very vague sense to M: "The mutual inductance M gives the magnetic coupling of the leakage fields between windings (flux in air)", but then go on to specify that "M does not have any relationship with the commonly used mutual inductance...". The branch inductance matrix of their equivalent circuit turns out to be completely filled, and its off-diagonal elements $M_{i,j}$ are determined by very complex formulae and have different signs, which raises further questions.

The reason for the above-described vacillations between "the lack of physical sense" and "physical interpretation" based on dubious 'postulates' is in the deeply rooted phenomenological approach to modeling the transformer by external characteristics with respect to its $n + 1$ poles (as a rule, by the short-circuit impedance between the pairs of its windings). This approach excludes the possibility of controlling the physical processes inside the transformer, in particular, the relationship between the magnetic fluxes in the individual parts of the magnetic circuit, the window, the space around the tank, etc., which is extremely important for assessing the magnetic state of the individual components of the magnetic circuit. As a result, the issues related to the analysis of electrodynamic stability of transformers in abnormal conditions remain unsolved. None of the existing theories, as well as the standard packages (Simulink Matlab, EMTR-type, etc.) developed on the basis of these theories, do not allow to even set the problem on assessing the differences in the saturation of the individual components of the magnetic circuit with a sudden short-circuit in one or more of the transformer windings (which is important for correctly assessing the initial short-circuit currents), as it is erroneously assumed that the magnetic circuit is not saturated in a short-circuit event (see [4, p. 307] or [8, p. 81], etc.).

At the same time, as shown in [13,14] for a double-winding transformer, implementing the idea of obtaining circuit models with all magnetic fluxes of the transformer displayed is possible (!) if *primary* quantities, i.e., the electric and magnetic field strengths and the Poynting vector, are used as a basis, and if the operating principles of the transformer are approached from a completely different perspective. The equivalent circuits with fluxes give physical sense to each of the circuit's elements. It turned out that *allocation of negative inductances* was required to display the magnetic fluxes in the equivalent circuit of even a double-winding transformer; besides, these inductances also play a key role in explaining the physics of magnetic super- and counter-fluxes under short-circuit conditions and in case of sudden short circuits. The existence of these fluxes was conclusively proved both experimentally [15] and by constructing images of the magnetic fields in a short-circuited transformer [16, 17].

The goal of this study is in obtaining similar 'physical' circuit models for a multi-winding shell-type transformer with a clear presentation of all magnetic fluxes between its windings, in the windings themselves, in the elements of the magnetic circuit, as well as between the magnetic circuit and the tank in case of saturation of steel (fig. 1). The term 'physical circuit models' is arbitrary and is used in order to:

– emphasize the fundamental difference between these models and the existing conventional equivalent circuits which in fact oversimplify the concept of an

n-winding transformer, describing it as a 'black box' with *n*+1 poles,

– reflect the universal character of the new models allowing, as a result of slight simplifications, to obtain the known equivalent circuits, as well as to control and correct the errors in any other models, for example, the ones proposed in [11].

Assumptions and notations. In accordance with the general rules [4,11], let us assume that all windings have been reduced to the same number of turns, i.e.,

$$w_a = w_b = w_c = w_d = w_e \to w_1 \qquad (1)$$

which allows to avoid using strokes that usually mark the reduced values. In describing the operating principles and the key features of any device, the secondary factors are initially neglected, and the device is regarded as a system with the optimal (limit) performance indicators, which the real device should approach. In our case, this means moving on to the analysis of the performance of the *n*-winding idealized transformer (fig. 1) with the following assumptions:

the magnetic circuit is characterized by $\mu_{stell} = \infty$ and the conductivity $\gamma_{stell} = \infty$;

the resistances of the windings $R_a = R_b = ... = R_e = 0$;

additional resistances for the steady state, caused by eddy currents in the windings, $R_a^{eddy} = R_b^{eddy} = ... = R_e^{eddy} = 0$;

winding height $h_w = h$, where h is the height of the transformer window;

the magnetic field lines in the window are straight and parallel to the core axis.

Fig. 1 shows the arbitrary positive directions of the magnetic fluxes. The absolute values of the flux complexes ($\dot{\Phi}_k$) coincide with their effective values (Φ_k). The typical relationship between the coil voltage and its flux has the form:

$$\dot{U}_k = j\omega w_1 \dot{\Phi}_k = k_0 \dot{\Phi}_k, \qquad (2)$$

where the constant

$$k_0 = j\omega w_1. \qquad (3)$$

The magnetic fluxes in the magnetic circuit (fig. 1):

$\dot{\Phi}_{leg}$ – in the *leg*;

$\dot{\Phi}_{side}$ – in the *side yoke*;

$\dot{\Phi}_j^a$ – in the *joint yoke* from the side of the leg towards the internal winding w_a;

$\dot{\Phi}_j^{a\delta}, \dot{\Phi}_j^{b\delta}, \dot{\Phi}_j^{c\delta}, \dot{\Phi}_j^{d\delta}$ – in the *joint yoke* from the side of the windings towards the gaps between the windings;

$\dot{\Phi}_j^{\delta b}, \dot{\Phi}_j^{\delta c}, \dot{\Phi}_j^{\delta d}, \dot{\Phi}_j^{\delta e}$ – in the *joint yoke* from the side of the gaps towards the windings;

$\dot{\Phi}_j^e$ – in the *joint yoke* from the side of the external winding w_e towards the side yoke.

The magnetic fluxes in the transformer window:

$\dot{\Phi}_{\delta 1}, \dot{\Phi}_{\delta 2}, \dot{\Phi}_{\delta 3}, \dot{\Phi}_{\delta 4}$ – in the channels between the windings;

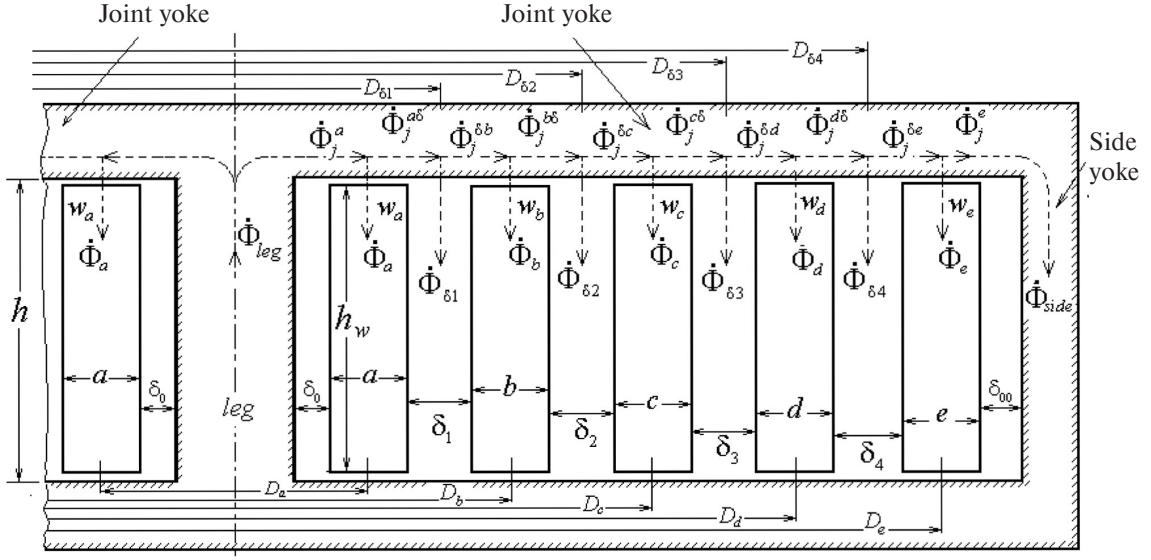

Fig. 1. Magnetic fluxes in the steel and in the window of a 5-winding shell transformer

$\dot{\Phi}_a, \dot{\Phi}_b, \dot{\Phi}_c, \dot{\Phi}_d, \dot{\Phi}_e$ – within the bulk of the windings.

Unlike the fluxes in the window of the idealized double-winding transformer, these fluxes are not in-phase and depend on the nature of the winding loads.

The following relations are obvious between the magnetic fluxes in the nodes of the magnetic circuit:

$$\dot{\Phi}_{leg} \equiv \dot{\Phi}_j^a = \dot{\Phi}_a + \dot{\Phi}_j^{a\delta}; \quad (4)$$

$$\dot{\Phi}_j^{a\delta} = \dot{\Phi}_{\delta 1} + \dot{\Phi}_j^{\delta b}; \quad (5)$$

$$\dot{\Phi}_j^{\delta b} = \dot{\Phi}_b + \dot{\Phi}_j^{b\delta}; \quad (6)$$

$$\dot{\Phi}_j^{b\delta} = \dot{\Phi}_{\delta 2} + \dot{\Phi}_j^{\delta c}; \quad (7)$$

$$\dot{\Phi}_j^{\delta c} = \dot{\Phi}_c + \dot{\Phi}_j^{c\delta}; \quad (8)$$

$$\dot{\Phi}_j^{c\delta} = \dot{\Phi}_{\delta 3} + \dot{\Phi}_j^{\delta d}; \quad (9)$$

$$\dot{\Phi}_j^{\delta d} = \dot{\Phi}_d + \dot{\Phi}_j^{d\delta}; \quad (10)$$

$$\dot{\Phi}_j^{d\delta} = \dot{\Phi}_{\delta 4} + \dot{\Phi}_j^{\delta e}; \quad (11)$$

$$\dot{\Phi}_j^{\delta e} = \dot{\Phi}_e + \dot{\Phi}_j^e \equiv \dot{\Phi}_e + \dot{\Phi}_{side}. \quad (12)$$

The principal idea of creating an *expanded* equivalent electrical circuit (in the sense that, along with the electrical values ($\dot{U}_1, \dot{U}_2, ..., \dot{U}_5$, $\dot{I}_1, \dot{I}_2, ..., \dot{I}_5$), it will display all of the above-listed magnetic fluxes, i.e., they can be *seen*) will be implemented through directly using these relations.

The magnetic resistances of the annular channels in the window:

$$R_{\delta 1}^M = \frac{h}{\mu_0 s_{\delta 1}}; \quad R_{\delta 2}^M = \frac{h}{\mu_0 s_{\delta 2}}; \quad R_{\delta 3}^M = \frac{h}{\mu_0 s_{\delta 3}}; \quad R_{\delta 4}^M = \frac{h}{\mu_0 s_{\delta 4}}. \quad (13)$$

where the lower index in the notation for the surface area (s_k) coincides with the notation for width of the corresponding annular channel:

$$s_{\delta 1} = \pi D_{\delta 1}\delta_1, \quad s_{\delta 2} = \pi D_{\delta 2}\delta_2, \quad s_{\delta 3} = \pi D_{\delta 3}\delta_3, \quad s_{\delta 4} = \pi D_{\delta 4}\delta_4. \quad (14)$$

The magnetic resistances of the annular channels occupied by the windings:

$$R_a^M = \frac{h}{\mu_0 s_a}; \quad R_b^M = \frac{h}{\mu_0 s_b}; \quad R_c^M = \frac{h}{\mu_0 s_c}; \quad R_d^M = \frac{h}{\mu_0 s_d}, \quad (15)$$

where

$$s_a = \pi D_a a, \quad s_b = \pi D_b b, \quad s_c = \pi D_c c, \quad s_d = \pi D_d d, \quad s_e = \pi D_e e. \quad (16)$$

These values are used to determine the terms that are part of the expression for the short-circuit (s/c) inductance of the corresponding pair of windings. For convenience of notation for the inductances, let us introduce a coefficient

$$\beta_0 = \frac{w_1^2 \mu_0}{h}. \quad (17)$$

To construct an equivalent circuit for a three-winding transformer with *a*,*b*,*c*-windings, we should consider the properties and characteristics of three 4T-shaped circuit models of double-winding transformers (*a*/*b*, *b*/*c* and *a*/*c*) that can be separated from it and essentially comprising it.

Negative inductances in a model of a double-winding transformer. In view of the notations introduced, the equivalent circuit of an idealized double-winding *a*,*b*-transformer takes the form shown in fig. 2,*a*. Fig. 2,*b* next to it shows the equivalent circuit for *a*, *b*,*c*-transformer.

a) *b*)

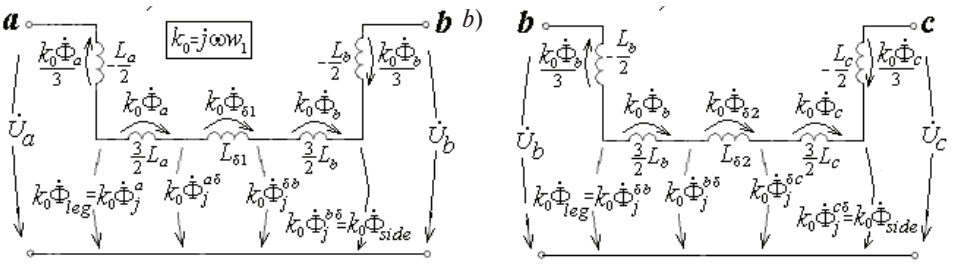

Fig. 2. 4T-shaped equivalent circuits of double-winding *a*,*b*- (*a*) and *b*,*c*- (*b*) transformers

In contrast with [13, 14], for the sake of convenience the branches with negative inductances are displayed vertically in both circuits. Both circuits are of the *reduced 4T- shaped*, as they contain four transverse arrows, each *highlighting* a magnetic flux in one of the parts of the magnetic circuit. Using Kirchhoff's second law, we can verify that Eqs. (4), (5), (6) hold in the circuit in Fig. 2a, and Eqs. (6), (7), (8) hold in the circuit in Fig. 2б. All inductances in the circuits (Figs. 2a, 2б) are series-connected. Their total value in each circuit is the typical short-circuit inductance (L^{sh}). For the circuit in fig. 2,*a*

$$L_{ab}^{sh} = L_a + L_{\delta 1} + L_b \qquad (18)$$

and for the circuit in fig. 2,*b*

$$L_{bc}^{sh} = L_b + L_{\delta 2} + L_c . \qquad (19)$$

However, unlike conventional theory (described in textbooks), the new theory [13, 14] regards each component of the short-circuit inductance not as a leakage inductance, but as a functional element of the equivalent circuit, or as a *means* for displaying the power flow (or the Poynting vector) through the corresponding segment of the transformer window. Because of this, the quantities

$$\begin{aligned} &L_{\delta 1} = \beta_0 s_{\delta 1};\ L_{\delta 2} = \beta_0 s_{\delta 2};\\ &L_{\delta 3} = \beta_0 s_{\delta 3};\ L_{\delta 4} = \beta_0 s_{\delta 4} \end{aligned} \qquad (20)$$

should be called the *inductance of power transportation* (or the inductance of *Poynting vector transportation*) *in the corridors between the windings* or just *corridor inductances*, while each of the quantities:

$$\begin{aligned} &L_a = \beta_0 \frac{s_a}{3};\ L_b = \beta_0 \frac{s_b}{3};\ L_c = \beta_0 \frac{s_c}{3};\\ &L_d = \beta_0 \frac{s_d}{3};\ L_e = \beta_0 \frac{s_e}{3} \end{aligned} \qquad (21)$$

should be called the *inductance of power flow increase* (or the *inductance of Poynting vector* increase), if it belongs to the primary winding, or the *inductance of power flow decrease* (or the *inductance of Poynting vector* decrease), if it belongs to the secondary winding.

The branches with negative inductances should be allocated in the equivalent circuit of the double-winding transformer for three reasons:

1) for localizing the fluxes passing through the bulk of the windings ($\dot{\Phi}_a$, $\dot{\Phi}_b$ in fig. 2,*a* and $\dot{\Phi}_b, \dot{\Phi}_c$ in fig. 2,*b*); these branches are then used to display the contribution of the fluxes in the bulk of the windings to their flux linkage (see formulae (57) and (58) in [14]);

2) to clearly demonstrate the super- and counter-fluxes in the magnetic circuit in case of a short circuit in one of the transformer's windings;

3) to conveniently implement the key idea of the paper, which is in constructing the equivalent circuits for multi-winding transformers by *stitching together* (combining) the circuit models of double-winding transformers.

Short-circuit super- and counter-fluxes are determined by comparing the s/c fluxes with the no-load flux ($\dot{\Phi}_o$) in the steel magnetic circuit which, in view of the assumptions made earlier, takes the same value in all parts of the magnetic circuit regardless of which of the windings (fig. 1) is powered by the primary voltage $\dot{U}_1$:

$$\dot{\Phi}_0 = \frac{\dot{U}_1}{k_0}. \qquad (22)$$

If only two windings are used in a 5-winding transformer, the other three can be regarded as measuring coils, which allows to assess the magnitudes of the super- and counter-fluxes in s/c modes of double-winding transformers.

Note 1. We are going to use the geometric dimensions of the windings for the 5-winding transformer (fig. 1), presented in [11], for our calculations (in millimeters):

$$a = 41,\ b = 43,\ c = 10,\ d = 10,\ e = 10,\ D_a = 438,$$
$$D_b = 578,\ D_c = 667,\ D_d = 723,\ D_e = 769,$$

$$\delta_1 = 28,\ \delta_2 = 18,\ \delta_3 = 18,\ \delta_4 = 13,\ D_{\delta 1} = 507,$$
$$D_{\delta 2} = 639,\ D_{\delta 3} = 695,\ D_{\delta 4} = 746,\ h = 979.$$

The number of turns of the winding is $w_1 = 100$.

The cross-sectional areas of the windings are then equal to (in m^2):

$$s_a = 0{,}0564;\ s_b = 0{,}0781;\ s_c = 0{,}0210;\ s_d = 0{,}0227;$$
$$s_e = 0{,}0242.$$

The cross-sectional areas of the gaps between the windings are then equal to (in m^2):

$$s_{\delta 1} = 0{,}0446;\ s_{\delta 2} = 0{,}0361;\ s_{\delta 3} = 0{,}0393;\ s_{\delta 4} = 0{,}0305.$$

According to (20) and (21), we obtain that (in mH):

$$L_{\delta 1} = 0{,}5724;\ L_{\delta 2} - 0{,}4638;\ L_{\delta 3} = 0{,}05044;$$
$$L_{\delta 4} = 0{,}03910;$$

$$L_a = 0{,}2413;\ L_b = 0{,}3340;\ L_c = 0{,}0896;$$
$$L_d = 0{,}0971;\ L_e = 0{,}1033.$$

Short-circuit resistances for the pairs of windings are obtained by Eqs. (18), (19) and similar ones (in mH):

$$L_{ab}^{sh} = 1{,}1479;\ L_{ac}^{sh} = 2{,}696;\ L_{ad}^{sh} = 3{,}1505;$$
$$L_{ae}^{sh} = 3{,}8393;\ L_{bc}^{sh} = 0{,}8876;\ L_{bd}^{sh} = 1{,}6685;$$
$$L_{be}^{sh} = 2{,}3573;\ L_{cd}^{sh} = 0{,}6913;\ L_{ce}^{sh} = 1{,}3801;$$
$$L_{de}^{sh} = 0{,}5916.$$

Let us consider an *a*,*b*-transformer (fig. 2, *a*). The other three windings (*c*,*d* and *e*) are open (fig. 1). Regardless of whether the winding *a* or *b* is the primary one, the s/c current is equal to

$$\dot{I}_{sh} = \frac{\dot{U}_1}{j\omega L_{ab}^{sh}} = \frac{\dot{U}_1}{j\omega(L_a + L_{\delta 1} + L_b)}. \qquad 23)$$

The *a*-winding is primary ($\dot{U}_1 = \dot{U}_a$), therefore the flux in the core

$$\dot{\Phi}_{leg}^{sh} \equiv \dot{\Phi}_j^{a\,sh} = \frac{\dot{U}_1 - \left(j\omega\left(-\frac{L_a}{2}\right)\right)\cdot \dot{I}_{sh}}{k_0} = \qquad (24)$$
$$= \frac{\dot{U}_1}{k_0}\left(1 + \frac{L_a}{2L_{ab}^{sh}}\right) = \left(1 + \frac{L_a}{2L_{ab}^{sh}}\right)\dot{\Phi}_0,$$

and the flux in the side yoke

$$\dot{\Phi}_{side}^{sh} \equiv \dot{\Phi}_j^{b\,sh} = \frac{\left(j\omega\left(-\frac{L_b}{2}\right)\right)\cdot \dot{I}_{sh}}{k_0} = \qquad (25)$$
$$= -\frac{\dot{U}_1}{k_0}\frac{L_b}{2L_{ab}^{sh}} = -\frac{L_b}{2L_{ab}^{sh}}\dot{\Phi}_0.$$

Since $\Phi_{leg}^{sh} > \Phi_0$, then the flux $\dot{\Phi}_{leg}^{sh}$ is the *super-flux*. Since $\dot{\Phi}_{side}^{sh}$ is directed towards the flux $\dot{\Phi}_{leg}^{sh}$, then $\dot{\Phi}_{side}^{sh}$ is the *counter-flux*. In our case, we obtain for the super-flux in the leg of the *a*,*b*-transformer:

$$\dot{\Phi}_{leg}^{sh} \equiv \dot{\Phi}_{leg}^{sh} = \left(1 + \frac{L_a}{2(L_a + L_{\delta 1} + L_b)}\right)\dot{\Phi}_0 =$$
$$= \left(1 + \frac{s_a}{2s_a + 6s_{\delta 1} + 2s_b}\right)\dot{\Phi}_0 = 1{,}105\dot{\Phi}_0.$$

Its counter-flux in the side yoke is equal to

$$\dot{\Phi}_{side}^{sh} = -\frac{L_b}{2(L_a + L_{\delta 1} + L_b)}\dot{\Phi}_0 =$$
$$= -\frac{s_b}{\left(2s_a + 6s_{\delta 1} + 2s_b\right)}\dot{\Phi}_0 = -0{,}146\dot{\Phi}_0.$$

All windings have the same number of turns, so the voltage readings in the *c, d, e* windings are identical and equal to:

$$\dot{U}_c^{sh} = \dot{U}_d^{sh} = \dot{U}_e^{sh} = k_0\dot{\Phi}_{side}^{sh} =$$
$$= -\frac{s_b}{\left(2s_a + 6s_{\delta 1} + 2s_b\right)}\dot{U}_1 = -0{,}146\,\dot{U}_1.$$

The first row of table 1 lists the numerical values of currents and voltages in the s/c mode under consideration at $\dot{U}_1 \equiv \dot{U}_a = 1000W$. The frequency $f = 50$ Hz was used when calculating the currents. The frequency is not involved in the ratios for fluxes and voltages. Designation **Tr.** from the word **Transformer**.

Table 1

Examples of calculating voltages and currents in the 5-winding transformer

Example	Quantity	Windings (fig. 1)				
		a	*b*	*c*	*d*	*e*
1	U_k (Volt)	1000	0	−146	−146	−146
(a,*b*-Tr.)	I_k^{sh} (Ampere)	2772,9	2772,9	0	0	0
2	U_k (Volt)	0	1000	1146	1146	1146
(*b*,*a*-Tr.)	I_k^{sh} (Ampere)	2772,9	2772,9	0	0	0
3	U_k (Volt)	940,7 (945,3)	1000 (1000)	1018 (1015,3)	1018 (1015,3)	1018 (1015,3)
(*b*,*a*-Tr.)						
$R_н = 1\Omega$	I_k^{sh} (Ampere)	940,7 (945,3)	940,7 (945,3)	0 (0)	0 (0)	0 (0)

Ending table 1

Example	Quantity	Windings (fig. 1)				
		a	*b*	*c*	*d*	*e*
4	U_k (Volt)	1000	445	0	−18,9	−18,9
(*a*, *c*- Tr.)	I_k^{sh} (Ampere)	1343,3	0	1343,3	0	0

Short-circuit super- and counter-fluxes in the same transformer change places if the *b*-winding is primary and $\dot{U}_1 = \dot{U}_b$ (i.e., in the *b*,*a*-transformer (fig. 2,*a*)). The current $\dot{I}_{sh}$ for the short-circuited *a*-winding coincides with its value (23), and the flux in the leg becomes the counter-flux:

$$\dot{\Phi}_{leg}^{sh} \equiv \dot{\Phi}_j^{a\,sh} = \frac{\left(j\omega\left(-\frac{L_a}{2}\right)\right)\cdot \dot{I}_{sh}}{k_0} = -\frac{\dot{U}_1}{k_0}\frac{L_a}{2L_{ab}^{sh}} = -\frac{L_a}{2L_{ab}^{sh}}\dot{\Phi}_0,$$

while the flux in the side yoke is transformed into the super-flux

$$\dot{\Phi}_{side}^{sh} \equiv \dot{\Phi}_j^{b\,sh} = \frac{\dot{U}_1 + j\omega\frac{L_b}{2}\cdot \dot{I}_{sh}}{k_0} = \frac{\dot{U}_1}{k_0}\left(1+\frac{L_b}{2L_{ab}^{sh}}\right) = \left(1+\frac{L_b}{2L_{ab}^{sh}}\right)\dot{\Phi}_0.$$

The voltage readings from the *c*, *d*, *e* windings will exceed the applied voltage, as shown in the second row of Table 1:

$$\dot{U}_c^{sh} = \dot{U}_d^{sh} = \dot{U}_e^{sh} = k_0\dot{\Phi}_{side}^{sh} = \left(1+\frac{s_b}{2s_a + 6s_{\delta 1} + 2s_b)}\right)\dot{U}_1 = 1{,}146\,\dot{U}_1,$$

thus confirming the occurrence of the s/c super-flux in the side yoke.

The third row of table 1 demonstrates that it is possible for a super-flux to emerge at a loud $R_н = 1\ \Omega$. The calculations are given in the Appendix.

Double-winding elements of the three-winding transformer. With the *d* and *e* windings open, the 5-winding transformer becomes a three-winding *a*,*b*,*c*-transformer. It contains three double-winding transformers: *a*,*b*-, *b*,*c*- and *a*,*c*-transformers (see figs. 2,*a*, 2,*b*, and 3,*a*).

In the schematic (*fig.* 3,*a*), L_a is the *inductance of power flow increase*, and L_c is the *inductance of power flow decrease*. Since the width of the corridor between the windings *a* and *c* is equal to

$$\delta_1 + b + \delta_2,$$

then the *inductance of power transportation in this corridor*

$$L_{\delta 1\,+\,b\,+\,\delta 2} = \beta_0(S_{\delta 1} + S_b + S_{\delta 2}). \qquad (26)$$

Taking into account (20) and (21), it can be represented as:

$$L_{\delta 1+b+\delta 2} = L_{\delta 1} + \frac{3}{2}L_b + \frac{3}{2}L_b + L_{\delta 2}. \qquad (27)$$

The magnetic flux in the corridor between the windings

$$\dot{\Phi}_{(\delta 1+b+\delta 2)} = \dot{\Phi}_{\delta 1} + \dot{\Phi}_b + \dot{\Phi}_{\delta 2} = \frac{j\omega L_{(\delta 1+b+\delta 2)}\dot{I}}{k_0}. \qquad (28)$$

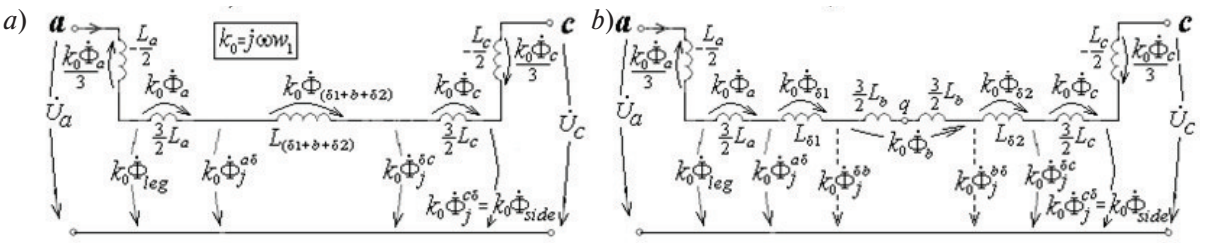

Fig. 3. 4T-shaped equivalent circuit of a double-winding *a*,*c*-transformer with the concentrated inductance $L_{\delta 1\,+\,b\,+\,\delta 2}$ (*a*) and its partition into four components with the central node *q* (*b*)

It follows from (27) and (28) that the flux in the bulk of the open *b*-winding is equal to

$$\dot{\Phi}_b = \frac{j\omega\left(\frac{3}{2}L_b + \frac{3}{2}L_b\right)\dot{I}}{k_0}, \qquad (29)$$

which is shown in fig. 3,*b*. It is also possible to identify the quantities $k_0\dot{\Phi}_j^{\delta b}$ and $k_0\dot{\Phi}_j^{b\delta}$ in the schematic, marked by dashed lines. The result is a 6T-shaped equivalent circuit of a double-winding transformer, which was a consequence of dividing the corridor between its *a* and *c* windings into three annular channels with the widths δ1, *b* and δ2.

Note 2. By partitioning the corridor into a larger number of channels, it is possible to construct an equivalent circuit with an arbitrary large number of transverse arrows, thus obtaining a *distributed* structure for the equivalent circuit of the double-winding transformer.

The internal inductance of the a,c-transformer (or the s/c inductance) from the side of the *a*-winding with the *c*-winding short circuited is equal to:

$$L_{ac}^{sh} = L_a + L_{\delta 1+b+\delta 2} + L_c = L_a + (L_{\delta 1} + 3L_b + L_{\delta 2}) +$$
$$+ L_c = L_{ab}^{sh} + L_b + L_{bc}^{sh} = 0{,}00237\,\text{H}.$$

Note 3. This expression implies a useful relation

$$L_b = L_{ac}^{sh} - (L_{ab}^{sh} + L_{bc}^{sh}) \qquad (30)$$

which will be used below when studying a three-winding transformer.

For the s/c current we obtain

$$\dot{I}_{sh} = \frac{\dot{U}_1}{j\omega L_{ac}^{sh}} = 1343{,}3\,\text{A}.$$

Similar to (24) and (25), we find the fluxes in the s/c mode:

$$\dot{\Phi}_{leg}^{sh} \equiv \dot{\Phi}_j^{a\,sh} = \left(1 + \frac{L_a}{2L_{ac}^{sh}}\right)\dot{\Phi}_0 =$$
$$= \left(1 + \frac{s_a}{2s_a + 6(s_{\delta 1} + s_b + s_{\delta 2}) + 2s_c}\right)\dot{\Phi}_0 = 1{,}051\dot{\Phi}_0;$$

$$\dot{\Phi}_{side}^{sh} \equiv \dot{\Phi}_j^{b\,sh} = -\frac{L_c}{2L_{ac}^{sh}}\dot{\Phi}_0 =$$
$$= -\frac{s_c}{2s_a + 6(s_{\delta 1} + s_b + s_{\delta 2}) + 2s_c} = -0{,}0189\dot{\Phi}_0.$$

They are weakened due to the fairly wide gap between the windings (see the last row of table 1). The voltages in the open windings *e*, *d* are equal to:

$$\dot{U}_e^{sh} = \dot{U}_d^{sh} = k_0\dot{\Phi}_{side}^{sh} = -0{,}0189\,\dot{U}_1.$$

The voltage at the terminals of the open *b*-winding can be found from its flux linkage

$$\dot{U}_b = j\omega\dot{\Psi}_b = k_0\left[(\dot{\Phi}_{leg} - \dot{\Phi}_a - \dot{\Phi}_{\delta 1}) - \frac{\dot{\Phi}_b}{2}\right]. \qquad (31)$$

In the s/c mode we obtain (see Table 1)

$$\dot{U}_b^{sh} = k_0\left[(\dot{\Phi}_{\text{ст}}^{sh} - \dot{\Phi}_a^{sh} - \dot{\Phi}_{\delta 1}^{sh}) - \frac{\dot{\Phi}_b^{sh}}{2}\right] =$$
$$= \left(1 + \frac{L_a}{2L_{ac}^{sh}} - \frac{\frac{3L_a}{2} + L_{\delta 1} + \frac{3L_b}{2}}{L_{ac}^{sh}}\right)\dot{U}_1 = 0{,}445\,\dot{U}_1.$$

Note. The s/c voltages listed in table 1 are presented as the consequences of the emergence of super- and counter-fluxes. This indicates that under real conditions the magnetic circuit is, firstly, unevenly magnetized in an s/c, and, secondly, its part containing the super-flux can turn out to be (depending on the cross-section of the magnetic circuit in this part) an order of magnitude more saturated than under the no-load conditions. With sudden short circuits this may lead to an increase in the initial s/c by 20-30% from its calculated value determined by the formulae of the conventional theory (known to have been derived in disregard of the magnetizing currents, i.e., assuming that the magnetic circuit is demagnetized in the event of an s/c (see [4, p. 307], [8, p.81 and p. 131], etc.)). The error up to 50% occurs in the calculations of electrodynamic forces under a short circuit.

A 6T-shaped equivalent circuit of an idealized three-winding transformer. Comparing the model of the double-winding *a*,*c*-transformer (fig. 3,b) with the two circuits in fig. 2, we can conclude that it can be regarded as the result of stitching the equivalent circuits of the *a*,*b*- and the *b*,*c*-transformers in node *q*. If we preserve the vertical branch with the negative inductance ($-L_b/2$), we obtain a three-pole circuit, which is the equivalent circuit of a three-winding (*a*,*b*,*c*)-transformer (fig. 4). The proof is in checking whether the *boundary conditions* that the three-winding transformer must satisfy are fulfilled in this scheme, that is to say, that the transformer must be simultaneously:

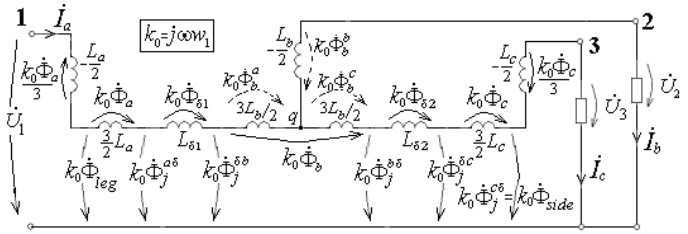

Fig. 4. 6T-shaped equivalent circuit of an idealized three-winding transformer

an *a*,*b*-transformer from the side of poles 1 and 2 (with pole 3 idle);

a *b*,*c*-transformer from the side of poles 2 and 3 (with pole 1 idle);

an *a*,*c*-transformer from the side of poles 1 and 3 (with pole 2 idle), which, obviously, follows from the above-described procedure of stitching the subcircuits along the negative inductance ($-L_b/2$). A fourth boundary condition is also satisfied, i.e., that the inductance ($-L_b/2$) is simultaneously included in the *a*,*b*- and the *b*,*c*-transformers. The circuit obtained also complies with the internal properties of the transformer both in the relationships between the fluxes and in the winding currents:

$$\dot{I}_a = \dot{I}_b + \dot{I}_c. \qquad (32)$$

The accuracy of the circuit (fig. 4) is confirmed by the fact that the inductances of the circuit branches emerging from node *q* coincide with the known expressions for L_{123}, L_{213} and L_{312} that have been first obtained in [1] as combinations of s/c resistances of separate double-winding transformers. In particular, we can write for the inductance of the branch between nodes 1 and *q* directly by the schematic (fig. 4), taking into account relation (30),

$$L_{1,q} = (L_a + L_{\delta 1} + L_b) + \frac{L_b}{2} =$$
$$= L^{sh}_{ab} + \frac{L^{sh}_{ac} - (L^{sh}_{ab} + L^{sh}_{bc})}{2} = \frac{L^{sh}_{ac} + L^{sh}_{ab} - L^{sh}_{bc}}{2} = L_{123},$$

where the penultimate fraction coincides with the expression for L_{123} from [4] after its indices *a*,*b*,*c* are substituted for 1,2,3, respectively. The inductance of the branch emerging from node *q* to node 2 of the central *b*-winding is negative and can be represented as

$$L_{2,q} = -\frac{L_b}{2} = -\frac{L^{sh}_{ac} - (L^{sh}_{ab} + L^{sh}_{bc})}{2} =$$
$$= \frac{L^{sh}_{ba} + L^{sh}_{bc} - L^{sh}_{ac}}{2} = L_{213} < 0.$$

For the inductance of the branch emerging from node *q* to node 3 of the external *c*-winding, we have

$$L_{3,q} = \frac{1}{2} L_b + (L_b + L_{\delta 2} + L_c) =$$
$$= \frac{L^{sh}_{ac} - (L^{sh}_{ab} + L^{sh}_{bc})}{2} + L^{sh}_{bc} = \frac{L^{sh}_{ac} + L^{sh}_{cb} - L^{sh}_{ab}}{2} = L_{312}.$$

When comparing these expressions with the known formulae, it should be borne in mind that in context, of course $L^{sh}_{pq} = L^{sh}_{qp}$.

Flux linkage in the central winding of the three-winding transformer. In an idealized three-winding transformer,

$$\dot{U}_1 = j\omega\dot{\Psi}_a = k_0\dot{\Psi}_a / w_1; \qquad (33)$$

$$\dot{U}_2 = j\omega\dot{\Psi}_b = k_0\dot{\Psi}_b / w_1; \qquad (34)$$

$$\dot{U}_3 = j\omega\dot{\Psi}_c = k_0\dot{\Psi}_c / w_1; \qquad (35)$$

It follows from these expressions and the circuit schematic (fig. 4) that the flux linkage in the windings can be written as:

$$\dot{\Psi}_a = w_1\dot{\Phi}_{leg} - \frac{w_1\dot{\Phi}_a}{3}; \qquad (36)$$

$$\dot{\Psi}_b = \frac{\dot{U}_2}{j\omega}; \qquad (37)$$

$$\dot{\Psi}_c = w_1\dot{\Phi}^{c\delta}_j + \frac{w_1\dot{\Phi}_c}{3} \to w_1\dot{\Phi}_{side} + \frac{w_1\dot{\Phi}_c}{3}. \qquad (38)$$

The arrow in the last expression indicates the equality of the fluxes $\dot{\Phi}^{c\delta}_j = \dot{\Phi}_{side}$ in the three-winding transformer. Expressions (36) and (38) coincide with formulae (57) and (58) in [14].

To expand (to open) expression (37), it is necessary to determine the voltages shown by the dashed arrows in fig. 4 and denoted as the product of k_0 by $\dot{\Phi}^a_b$, $\dot{\Phi}^c_b$ and $\dot{\Phi}^b_b$. It follows from the circuit that are related through a system of equations

$$\dot{\Phi}_b^a + \dot{\Phi}_b^c = \dot{\Phi}_b; \quad (39)$$

$$k_0\dot{\Phi}_b^a = j\omega\frac{3}{2}L_b\dot{I}_a; \quad (40)$$

$$k_0\dot{\Phi}_b^c = j\omega\frac{3}{2}L_b\dot{I}_c, \quad (41)$$

whence it follows that

$$\dot{\Phi}_b^a = \frac{\dot{I}_a}{\dot{I}_a + \dot{I}_c}\dot{\Phi}_b; \quad (42)$$

$$\dot{\Phi}_b^c = \frac{\dot{I}_c}{\dot{I}_a + \dot{I}_c}\dot{\Phi}_b. \quad (43)$$

Then it follows from the expression for the voltage

$$k_0\dot{\Phi}_b = j\omega\frac{3}{2}L_b\dot{I}_a + j\omega\frac{3}{2}L_b\dot{I}_c \quad (44)$$

that

$$j\omega\frac{L_b}{2} = \frac{k_0\dot{\Phi}_b}{3(\dot{I}_a + \dot{I}_c)}, \quad (45)$$

and we obtain for the voltage in the vertical branch

$$k_0\dot{\Phi}_b^b = j\omega\frac{L_b}{2}\dot{I}_b = \frac{\dot{I}_b}{\dot{I}_a + \dot{I}_c}\,\frac{k_0\dot{\Phi}_b}{3} \quad (46)$$

or

$$k_0\dot{\Phi}_b^b = \frac{\dot{I}_a - \dot{I}_c}{\dot{I}_a + \dot{I}_c}\,\frac{k_0\dot{\Phi}_b}{3}. \quad (47)$$

As a result, the voltage in the terminals of the central winding can be represented as

$$\dot{U}_2 = k_0\dot{\Phi}_j^{\delta b} - k_0\dot{\Phi}_b^a + k_0\dot{\Phi}_b^b =$$
$$= k_0\dot{\Phi}_j^{\delta b} - \frac{\dot{I}_a}{\dot{I}_a + \dot{I}_c}k_0\dot{\Phi}_b + \frac{\dot{I}_a - \dot{I}_c}{\dot{I}_a + \dot{I}_c}\cdot\frac{k_0\dot{\Phi}_b}{3}.$$

Taking into account (3), (32) and (37), we obtain the formula for the desired flux linkage:

$$\dot{\Psi}_b = w_1\dot{\Phi}_j^{\delta b} - \frac{\dot{I}_a - \frac{\dot{I}_b}{3}}{\dot{I}_a + \dot{I}_c}w_1\dot{\Phi}_b. \quad (48)$$

A 6T-shaped equivalent circuit of a real three-winding transformer. Ref. [14] examined in great detail the technique of enhancing the circuit model of the idealized transformer by the winding resistances and the *transverse branches* to take into account the active and reactance losses in the steel, including the sections between the tank and the magnetic circuit parts, in order to obtain the equivalent circuit of a real double-winding transformer. Similarly, the idealized model (fig. 4) can be substituted by the equivalent circuit of a real three-winding transformer, as shown by the dashed lines in fig. 5. The notations for the added inductances and fluxes correspond to the ones adopted in [14]. Nonlinear inductances and the conductivities parallel-connected to them correspond to:

L_{leg}, g_{leg} to the leg in which the flux $\dot{\Phi}_{leg}$ flows (fig. 1);

$L_j^{a\delta}$, $g_j^{a\delta}$ to the part of the joint yoke in which the flux $\dot{\Phi}_j^{a\delta}$ flows;

$L_j^{\delta b}$, $g_J^{\delta b}$, to the part of the joint yoke in which the flux $\dot{\Phi}_j^{\delta b}$ flows, etc.

The linear inductances series-connected to them are introduced to take into account the magnetic fluxes occurring due to the finite permeability of steel or its saturation. They correspond to:

$L_{\delta 0} = \mu_0 s_{\delta 0} w_1^2 / h$ to the segment with the width δ_0 between the leg and the internal *a*-winding, in which the flux $\dot{\Phi}_{\delta 0}$ flows (fig. 1);

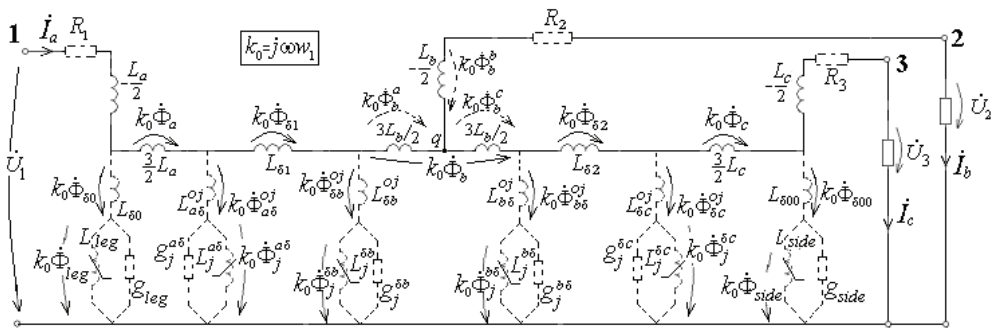

Fig. 5. 6T-shaped equivalent circuit of a real three-winding transformer

$L^{oj}_{a\delta} = \mu_0 s^{oj}_{a\delta} w_1^2 / l^{oj}_{a\delta}$ to the segment with the surface area $s^{oj}_{a\delta}$ and the length $l^{oj}_{a\delta}$ between the joint yoke and the tank, in which the flux $\dot{\Phi}^{oj}_{a\delta}$ flows parallel to the flux $\dot{\Phi}^{a\delta}_{J}$ in the joint yoke;

$L^{oj}_{\delta b} = \mu_0 s^{oj}_{\delta b} w_1^2 / l^{oj}_{\delta b}$ to the segment with the surface area $s^{oj}_{\delta b}$ and the length $l^{oj}_{\delta b}$ between the joint yoke and the tank, in which the flux $\dot{\Phi}^{oj}_{\delta b}$ flows parallel to the flux $\dot{\Phi}^{\delta b}_{j}$ in the yoke, etc.

Note 4. The circuit (fig. 5) should also be complemented with the resistances R^{eddy}_a, R^{eddy}_b, R^{eddy}_c by dividing each of them into a positive and a negative part, for example,

$$R^{eddy}_b = \frac{3}{2} R^{eddy}_b + \left(-\frac{R^{eddy}_b}{2} \right). \qquad (49)$$

The resistance $3R^{eddy}_b / 2$ should be series-connected with the inductances $3L_b / 3$, and the negative resistance $\left(-R^{eddy}_b / 2\right)$ should be series-connected with the inductance ($-L_b / 2$). This technique is substantiated in [6, p.87]. As a result, the circuit will obtain seven additional resistances for taking into account the eddy currents in the windings. The winding resistances R_a, R_b, R_c should be divided similarly. They are not shown in the schematic, so as not to overload fig. 5.

Note 5. The negative inductances in the equivalent circuits are typically regarded as a 'minor' hindrance (*a thorn in the side*). Monograph [6], specifically dedicated to multi-winding transformers, mentioned the negative inductance briefly in seven lines. Ref. [5, p. 125] goes as far as to suggest 'to disregard the negative inductances for the modes with high saturation of steel'. However, it follows from the equivalent circuit (fig. 5) that this can lead to an increased error in calculating the super-fluxes in a short-circuited transformer. Indeed, assuming for the sake of simplicity that in this case only the leg is saturated in the event of an s/c, we obtain a circuit (fig. 5) with a left transverse branch whose voltage can be represented as:

$$k_0 \dot{\Phi}^{sh}_{leg} + k_0 \dot{\Phi}^{sh}_{\delta 0} = \dot{U}_1 - \left(-j\omega \frac{L_a}{2} \right) \dot{I}^{sh}_a . \qquad (50)$$

The s/c current $\dot{I}^{sh}_a$ is high. The second term in the right-hand side of this expression is also fairly substantial. This is why neglecting it will lead to a substantial error in determining the super-flux $\dot{\Phi}^{sh}_{leg}$ in the core. It follows from (50) that the value of the super-flux in a saturated short-circuited transformer exceeds that in an unsaturated transformer.

A 2*n*T-shaped equivalent circuit of an *n*-winding idealized transformer. The above-described method of stitching 4T-shaped models of double-winding transformers is fully applicable to designing an equivalent circuit for any *n*-winding transformer. As an example, fig. 6 shows an equivalent circuit of an idealized 5-winding transformer. The number of transversal voltage arrows (with the fluxes) in the circuit is equal to 2*n*, which gave reason to call it the 2*n*T-shaped model. The total number of negative inductances in the circuit is equal to the number of windings, in this case, five. Any winding or group of windings can be regarded as primary, the rest of the windings as secondary ones. The *a*-winding acts as primary in the schematic in fig. 6. To obtain the model of the real transformer, the circuit in fig. 6 should be complemented by transverse branches taking into account the losses in the steel, as well as the resistances, as described in Note 4.

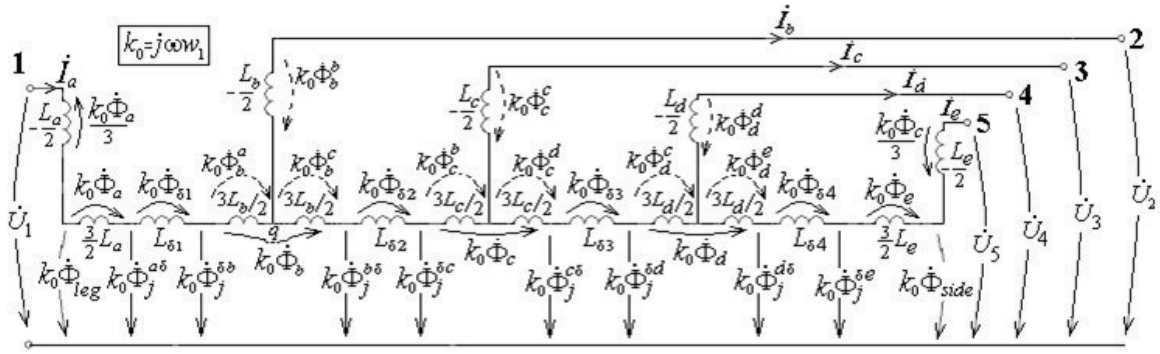

Fig. 6. Equivalent circuit of a 5-winding transformer

Transformation of negative inductances of the internal windings into mutual inductances. Negative inductances can be eliminated by transferring them across the nodes. According to the rules of these transformations [18], when transferring, for example, the inductance $(-L_b / 2)$ across node q (fig. 6), its value should be added to both inductances $3L_b / 2$ (after which they will be equal to L_b) and the mutual inductance, equal to $M_b = L_b / 2$, should be introduced between them, as shown in fig. 7. The negative inductances of two other internal windings $(-L_c / 2)$ and $(-L_d / 2)$ have been transferred in a similar manner, and two new mutually inductive couplings $M_c = L_c / 2$ and $M_d = L_d / 2$ have appeared in the circuit. With the labeling adop-ted for the schematic in fig. 7, all mutual inductances are positive.

Negative inductances of the external windings $(-L_a / 2)$ and $(-L_e / 2)$ have been preserved, thus ensuring that all transverse voltages remain the same as in the circuit (fig. 6). Therefore, the circuit in Fig. 7 can also be converted into a circuit of a real transformer by adding transverse and longitudinal branches which take into account the additional resistance and reactance losses, as described above for the circuit in fig. 6.

A compact ladder equivalent circuit for an idealized transformer without negative inductances. Combining the series-connected inductances between the nodes of the circuit in fig. 7, we obtain the circuit in fig. 8 with positive inductances equal to the s/c inductances of the corresponding double-winding transformers. In particular, by summing up the inductances between node 1 and node q, in view of (18), we have

$$-\frac{L_a}{2} + \frac{3}{2}L_a + L_{\delta 1} + L_b = L_{ab}^{sh}.$$

Similarly, for the group of series-connected inductances to the right of node q, based on (19), we find

$$L_b + L_{\delta 2} + L_c = L_{bc}^{sh},$$

and so on. As a result, we obtain a compact ladder equivalent circuit of an idealized equivalent n-winding transformer, described by a symmetric tridiagonal inductance matrix **L** shown in fig. 8. However, the opportunities for monitoring the fluxes, including the super- and counter-fluxes in case of an s/c, are lost for this circuit. The accuracy of the circuit model (fig. 8) is partially confirmed by the fact that the solutions to the examples in table 1 found using this model coincide with the numerical data for the voltage currents in table 1, previously obtained from the analysis of super- and counter fluxes.

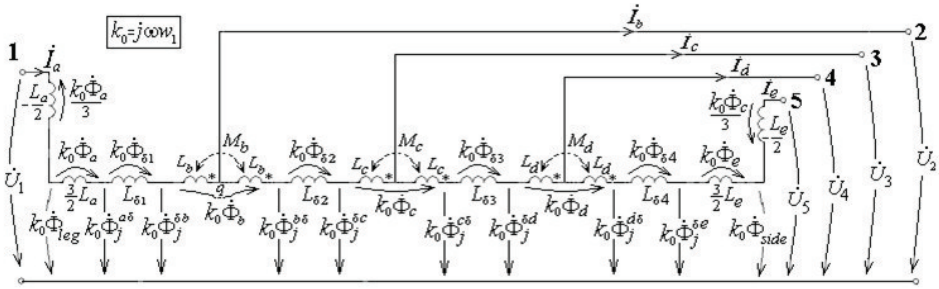

Fig. 7. Equivalent circuit of a 5-winding transformer without negative inductances of the internal windings

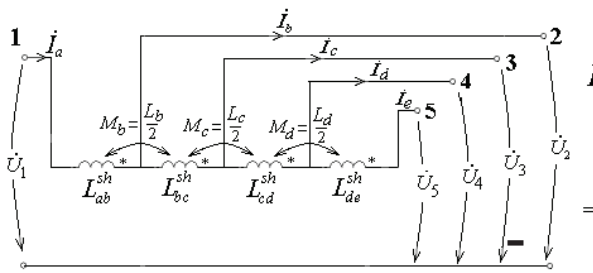

$$\boldsymbol{L} = \begin{pmatrix} L_{ab}^{sh} & M_b & 0 & 0 \\ M_b & L_{bc}^{sh} & M_c & 0 \\ 0 & M_c & L_{cd}^{sh} & M_d \\ 0 & 0 & M_d & L_{de}^{sh} \end{pmatrix} =$$

$$= \begin{pmatrix} 1{,}1479 & 0{,}1671 & 0 & 0 \\ 0{,}1671 & 0{,}8876 & 0{,}04428 & 0 \\ 0 & 0{,}04428 & 0{,}6913 & 0{,}04859 \\ 0 & 0 & 0{,}04859 & 0{,}5916 \end{pmatrix} \times 10^{-3} H$$

Fig. 8. Compact ladder equivalent circuit of the idealized 5-winding transformer with s/c resistances and its tridiagonal inductance matrix

The structure of the compact circuit (fig. 8) coincides with the topology of the model in [11], but differs from it by the elements of the matrix **L** which is completely filled in Ref. [11], as, according to the hypothesis of the authors, mutual inductances $M_{i,j}$ should supposedly hold between all inductances of the circuit's branches. The physical interpretation of these mutual inductances seems rather artificial, as hey exhibit alternating signs. In contrast to [11, 12], this paper presented a compact model (fig. 8) based on the rigorous methods of circuit theory instead of conjecture and hypotheses. All off-diagonal elements of the matrix **L** are positive, which follows from the very method used for obtaining them.

Conclusion. We have obtained a new ladder equivalent circuit of an *n*-winding transformer, allowing to fully represent the physical picture of the processes occurring in it by displaying the paths of the magnetic fluxes and their values in the circuit. A key feature of the designed circuit is its modular structure resulting from stitching simpler circuit models of conventional double-winding transformers. Unlike previous meaningless assessments of the negative inductances as "referencing the equivalent circuit of the *n*-winding transformer with the real relations", this paper regards them as elements of the circuit playing a key role in displaying the magnetic fluxes, which is important for the developers of standard software packages for correctly simulating and refining the processes occurring in a multi-winding transformer in abnormal operation modes. It was rigorously proved that the equivalent circuit of an *n*-winding transformer with mutual inductances introduced instead of the negative ones is characterized by a three-diagonal matrix of positive inductances. The circuits described can be used for the analyzing both steady-state and dynamic processes.

Appendix

It seems interesting to evaluate the fluxes and voltages in the presence of a small resistive load $R = 1\ \Omega$ in a *b*,*a*-transformer (fig. 2,*a*) at $\dot{U}_1 = \dot{U}_b = 1000V$ and compare the results with the data obtained in [11, p. 360] for this case. It follows directly from the circuit in fig. 2,*a* that the current

$$\dot{I} = \frac{\dot{U}_b}{R + j\omega L_{ab}^{sh}} = \frac{\dot{U}_1}{R + j\omega(L_a + L_{\delta 1} + L_b)} = (884{,}9 - j319{,}1)\,\text{A},$$

the absolute value of the current $I = 940{,}7$ A. The voltage for the load $R = 1\ \Omega$ is equal to

$$\dot{U}_a = R\dot{I} = (884{,}9 - j319{,}1)\,\text{V}$$

and, consequently, $U_a = 940{,}7$ V. We can write for the flux in the core

$$\dot{\Phi}_{leg} \equiv \dot{\Phi}_j^a = \frac{\left(R - j\omega\frac{L_a}{2}\right)\cdot \dot{I}_{sh}}{k_0} = \frac{\dot{U}_1}{k_0}\frac{\left(R - j\omega\frac{L_a}{2}\right)}{(R + j\omega L_{ab}^{sh})} = \frac{\left(R - j\omega\frac{L_a}{2}\right)}{(R + j\omega L_{ab}^{sh})}\dot{\Phi}_0 = (0{,}873 - j0{,}353)\dot{\Phi}_0,$$

and, consequently, $\Phi_{leg} \equiv \Phi_j^a = 0{,}941\Phi_0$. It also follows directly from the circuit in Fig. 2*a* that the flux in the side yoke is equal to

$$\dot{\Phi}_{side} \equiv \dot{\Phi}_j^b = \frac{\dot{U}_b - j\omega\left(-\frac{L_b}{2}\right)\cdot \dot{I}}{k_0} = \frac{\dot{U}_1}{k_0}\left(1 + \frac{j\omega L_b}{2(R + j\omega L_{ab}^{sh})}\right) = \left(1 + \frac{j\omega L_b}{2(R + j\omega L_{ab}^{sh})}\right)\dot{\Phi}_0 = (1{,}0167 + j0{,}0464)\dot{\Phi}_0$$

and since $\Phi_{side} \equiv \Phi_j^b = 1{,}018\Phi_0$, it can be regarded as a super-flux. The voltages in the windings *c*, *d*, *e* are equal to

$$\dot{U}_c = \dot{U}_d = \dot{U}_e = k_0\dot{\Phi}_{side} = \left(1 + \frac{j\omega L_b}{2(R + j\omega L_{ab}^{sh})}\right)\dot{U}_1 = 1{,}018\,\dot{U}_1$$

and exceed by modulus the applied voltage (see row 3 in table 1). The values obtained in [11] are listed in brackets. The reason for the discrepancy between the calculated results and the data of [11] is that the conditions for calculating the s/c voltages are formulated imprecisely in [11, p. 354].

REFERENCES

1. **Boyajian A.** Theory of three circuit transformers. – *AIII Trans*. Feb. 1924, P. 208–528.

2. **Starr F.** Equivalent circuits – I. *AIII Trans*. Jan. 1932. Vol 57. P. 287–298.

3. **Blume L.F., Boyajian A., Gamilly G., Lenox T.C. Minnec S. Montsinger M. V.** Transformer Engineering: A treatise on the Theory, Operation and Application of Transformer. New York: Wiley, 1951. 239 p.

4. **Vasyutinskii, S. B.** Theory and calculation of power transformers. Leningrad: Energiya, 1970. 432 s.

5. **Leites L.V.** Electromagnetic calculations of transformers and reactors. M.: Energy, 1981. 392 s.

6. **Leites L.V., Pinczow A.M.** An equivalent circuit of a multi-winding transformers. M.: Energy, 1974. 192 s.

7. **Petrov G.N.** The electric machine. Part 1. M.: Energy, 1974. 240 s.

8. **Ivanov-Smolensky, A.V.** Electrical machines. M.: Energy , 1980. 927 s.

9. **Hnikov A.V.** Theory and calculation of multiple-winding transformers. Publishing house: Solon-press, 2003. 114 p.

10. **Voldek A.I., Popov V.V.** Electric machine. Introduction to electromechanics. Machines of direct-current and transformers. St. Petersburg: Piter, 2007. 320 s.

11. **Alvarez-Marino C., Leon F., Lopez-Fernandez X.M.** Equivalent Circuit for the Leakage Inductance of Multiwinding Transformers: Unification of terminal and duality models. *IEEE transactions on power delivery*. Jan. 2012. Vol. 27. N° 1. P. 353–361.

12. **Leon F., Martinez J.A.** Dual Three-winding Transformer Equivalent Circuit matching Leakage measurements. *IEEE transactions on power delivery*. January 2009. Vol. 24. № 1. P. 160–168.

13. **Shakirov M.A.** The Poynting Vector and the new theory of transformers. Part 1. *Electricity*. 2014. № 9. S. 52–59 (rus.)

14. **Shakirov A.M.** The Poynting vector and the new theory of transformers. Part 2. *Electricity*. 2014. Vol. 10. P. 53–65. (rus.)

15. **Shakirov M.A., Andrushchuk V.V., Duan Lijun**. Anomalous magnetic fluxes in two-winding transformer under short circuit conditions. *Electricity*. 2010. № 3. P. 55–63. (rus.)

16. **Shakirov M.A., Varlamov V.Yu.** Patterns of magnetic SVER – and anti-stream in a short-circuited winding of the transformer. Part 1. Armour transformer. *Electricity*. 2015. № 8. S. 9–19. (rus.)

17. **Malygin V.M.** Lokalization of the Energy flux in the transformer. *Electricity*. 2015. № 4. S. 60–65. (rus.)

18. **Shakirov M.A.** Conversion and diakoptic electrical circuits. Leningrad: Publishing house of Leningrad. University press, 1980. 196 S.

СПИСОК ЛИТЕРАТУРЫ

1. **Boyajian A.** Theory of three circuit transformers. – *AIII Trans*. Feb. 1924, P. 208–528.

2. **Starr F.** Equivalent circuits – I. *AIII Trans*. Jan. 1932. Vol 57. P. 287–298.

3. **Blume L.F., Boyajian A., Gamilly G., Lenox T.C. Minnec S. Montsinger M. V.** Transformer Engineering: A treatise on the Theory, Operation and Application of Transformer. New York: Wiley, 1951. 239 p.

4. **Васютинский С.Б.** Вопросы теории и расчета трансформаторов. Л.: Энергия, 1970. 432 с.

5. **Лейтес Л.В.** Электромагнитные расчеты трансформаторов и реакторов. М.: Энергия, 1981. 392 с.

6. **Лейтес Л.В., Пинцов А.М.** Схемы замещения многообмоточных трансформаторов. М.: Энергия, 1974. 192 с.

7. **Петров Г.Н.** Электрические машины. Часть 1. М.: Энергия, 1974. 240 с.

8. **Иванов-Смоленский А.В.** Электрические машины. М.: Энергия, 1980. 927 с.

9. **Хныков А.В.** Теория и расчет многообмоточных трансформаторов. Изд-во.: Солон-пресс, 2003. 114 с.

10. **Вольдек А.И., Попов В.В.** Электрические машины. Введение в электромеханику. Машины постоянного тока и трансформаторы. СПб: Питер, 2007. 320 с.

11. **Alvarez-Marino C., Leon F., Lopez-Fernandez X.M.** Equivalent Circuit for the Leakage Inductance of Multiwinding Transformers: Unification of terminal and duality models // IEEE transactions on power delivery. Jan. 2012. Vol. 27. № 1. P. 353–361.

12. **Leon F., Martinez J.A.** Dual Three-winding Transformer Equivalent Circuit matching Leakage measurements // IEEE transactions on power delivery. January 2009. Vol. 24. № 1. P. 160–168.

13. **Шакиров М.А.** Вектор Пойнтинга и новая теория трансформаторов. Часть 1 // Электричество. 2014. № 9. С. 52–59.

14. **Шакиров М.А.** Вектор Пойнтинга и новая теория трансформаторов. Часть 2 // Электричество. 2014. № 10. С. 53–65.

15. **Шакиров М.А., Андрущук В.В., Дуан Лиюн.** Аномальные магнитные потоки в двухобмоточном трансформаторе при коротком замыкании // Электричество. 2010. № 3. С. 55–63.

16. **Шакиров М.А., Варламов Ю.В.** Картины магнитных сверх- и антипотоков в короткозамкнутом двухобмоточном трансформаторе. Часть 1. Броневой трансформатор // Электричество. 2015. № 8. С. 9–19.

17. **Малыгин В.М.** Локализация потока энергии в трансформаторе (по поводу статьи М.А. Шакирова, “Электричество”, 2014, № 9 и 10) // Электричество. 2015. № 4. С. 60–65.

18. **Шакиров М.А.** Преобразования и диакоптика электрических цепей. Л.: Изд-во Ленингр. ун-та, 1980. 196 с.

СВЕДЕНИЯ ОБ АВТОРАХ/AUTHORS

SHAKIROV Mansur A. – Peter the Great St. Petersburg Polytechnic University.
29 Politechnicheskaya St., St. Petersburg, 195251, Russia.
E-mail: manshak@mail.ru

ШАКИРОВ Мансур Акмелович – доктор технических наук профессор Санкт-Петербургского политехнического университета Петра Великого.
195251, Россия, г. Санкт-Петербург, Политехническая ул., 29.
E-mail: manshak@mail.ru